Extreme flood events at higher temperatures exacerbate the loss of soil functionality and trace gas emissions in grassland

Rafael Sanchez-Rodriguez, Antonio; Nie, Chengrong; Hill, Paul W.; Chadwick, David R.; Jones, Davey L.

Soil Biology and Biochemistry

DOI:
10.1016/j.soilbio.2018.12.021

Published: 01/03/2019

Peer reviewed version

Accepted Manuscript

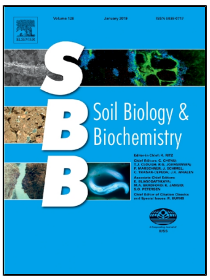

Extreme flood events at higher temperatures exacerbate the loss of soil functionality and trace gas emissions in grassland

Antonio Rafael Sánchez-Rodríguez, Chengrong Nie, Paul W. Hill, David R. Chadwick, Davey L. Jones

PII:	S0038-0717(18)30439-5
DOI:	10.1016/j.soilbio.2018.12.021
Reference:	SBB 7373
To appear in:	*Soil Biology and Biochemistry*
Received Date:	20 August 2018
Accepted Date:	20 December 2018

Please cite this article as: Antonio Rafael Sánchez-Rodríguez, Chengrong Nie, Paul W. Hill, David R. Chadwick, Davey L. Jones, Extreme flood events at higher temperatures exacerbate the loss of soil functionality and trace gas emissions in grassland, *Soil Biology and Biochemistry* (2018), doi: 10.1016/j.soilbio.2018.12.021

Extreme flood events at higher temperatures exacerbate the loss of soil functionality and trace gas emissions in grassland

Antonio Rafael Sánchez-Rodríguez[a,b,*], Chengrong Nie[a,c], Paul W. Hill[a], David R. Chadwick[a], Davey L. Jones[a,d]

[a] *Environment Centre Wales, Bangor University, Gwynedd LL57 2UW, UK*

[b] *Departamento de Agronomía, Universidad de Córdoba, ETSIAM, Córdoba, Andalucía 14071, Spain*

[c] *School of Food Science & Technology, Foshan University, Foshan 528231, Guangdong Province, China*

[d] *UWA School of Agriculture and Environment, University of Western Australia, Crawley, WA 6009, Australia*

*Corresponding author. Tel.: +34 957218915

E-mail address: antonio.sanchez@uco.es (A.R. Sánchez-Rodríguez).

Abstract

The frequency and intensity of extreme weather events (e.g. flood, drought) are predicted to increase for the foreseeable future and it is expected that these will negatively impact upon agroecosystem functioning. Our understanding of how grassland ecosystems respond to extreme weather events occurring at different times of the year, however, is lacking. To better understand the seasonal response of grassland to flooding, we subjected an agricultural grassland to an 8-week extreme flood event at three different temperatures (5 °C-winter, 15 °C-spring/autumn and 25°C-summer) and then followed its subsequent recovery for 9 weeks after floodwater removal. We focused on key indicators of ecosystem functioning including primary production, nutrient cycling, greenhouse gas (GHG) emissions, ammonia (NH_3) volatilization, and soil microbial communities. The experiment used intact soil mesocosms (1 kg) with indigenous vegetation collected from a grassland with no previous history of flooding. Flooding reduced biomass production by 18% at 5 °C, 50% at 15 °C and 95% at 25 °C. Flooding also significantly disrupted elemental cycling (nitrogen, phosphorus and carbon) as evidenced by an increased release of P, Fe and NH_4^+ into the soil and overlying floodwater and large amounts of CH_4 and NH_3 released to the atmosphere (mainly during the flooding). These effects were more pronounced at higher temperatures (e.g. 45 to 700 kg CH_4-C ha^{-1} and 1 to 5 kg NH_3-N ha^{-1} at 15 and 25 °C, respectively). In addition, after floodwater removal this NH_4^+ was rapidly nitrified leading to large losses of N_2O (1.0 to 14.2 kg N_2O-N ha^{-1} at 5 to 25 °C, respectively). Especially at higher temperatures, flooding resulted in a reduction in soil microbial biomass (more than 58% of the equivalent unflooded treatment at 25 °C) and changes in microbial community structure (assessed by PLFAs). Further, some of these changes persisted after flood removal including a loss of actinomycetes, arbuscular mycorrhizal fungi and fungi. Overall, we conclude that ecosystem responses to extreme weather events are critically dependent on temperature with those occurring at higher temperatures having a greater negative impact than those at the lowest temperature (5 °C). The large potential release of CH_4 and N_2O also suggests that flood events should be considered as a potential source of GHGs when comparing top-down and bottom-up calculations

of national inventories, and that further work is needed to better refine GHG emission estimates for these events.

Keywords: Climate change, Nitrous oxide, Methane, Iron oxyhydroxide; PLFA; Soil microorganisms

1. Introduction

Climate change is increasing the incidence of extreme weather events (Slater and Villarini, 2016) and current predictions indicate that their frequency and intensity will increase for the foreseeable future (IPCC, 2014). These events constitute a major threat to the delivery of soil-related agroecosystem services such as biomass production, biodiversity conservation, erosion control, pest and disease control, water quality and supply, and climate regulation, resulting in a loss of soil functioning (Bünemann et al., 2018).

Under future global warming scenarios, increases in temperature will result in more intense rainfall events (a warmer atmosphere can hold more water), an acceleration of snow and ice melt, and an increase in sea level, thereby increasing the risk of flooding (Trenberth, 2011). It is also predicted that areas with no previous history of flooding will become increasingly affected (Thorne, 2014). Extreme flood events can occur throughout the year and can cover large land areas with floodwater persisting from days to months, with floodwater depths reaching up to 2 m (Met Office, 2014; Morris and Brewin, 2014; Posthumus et al., 2009; Romanescu and Stoleriu, 2017). The overall damage to agroecosystems appears to be dependent upon the time of year when floods occur (Posthumus et al., 2009), plant species and their growth stage (Morris and Brewin, 2014), the type of flooding and the preceding agricultural management regime (Sánchez-Rodríguez et al., 2017, 2018b). At higher temperatures, chemical and biological soil reactions are accelerated and it is normally assumed that these will aggravate the effects of extreme flood events on plant production (Posthumus et al., 2009) and potential nutrient losses (Sánchez-Rodríguez et al., 2018b), however, colder weather also causes devastating effects if the crop is completely submerged (Das et al., 2009). It is also important to note that the impact of flooding on soil-based ecosystem services may continue after the floodwater has receded (Niu et al., 2014; Osanai et al., 2017).

Greenhouse gas (GHG) emissions from agricultural soils are likely to markedly shift in response to extreme weather events. For example, drought is expected to reduce GHG emissions as microbial activity becomes water-limited, whilst in contrast, flooding may increase net GHG emissions, due to a microbial switch from aerobic to anaerobic metabolism (Hou et al., 2000). Although N_2O produced under aerobic conditions may be reduced, and CH_4 emissions may increase under flooding, the overall mineralization of soil organic carbon (SOC) is typically suppressed due to the lack of O_2 required for oxidative-based enzymatic processes (Miller et al., 2001). Interestingly, however, there is also evidence showing an increase in mineralization in waterlogged or flooded soils (Alongi et al., 2012), particularly at elevated temperatures (Kirwan and Blum, 2011) when N and C, factors that limit decomposition rates of organic matter, are abundant.

In relation to plant biomass production and water quality, the release of nutrients and consequent loss of soil fertility may also be aggravated under prolonged inundation, altering the cycling of key nutrients (e.g. N, P, S; Bünemann et al., 2018). For example, under flooding and progressive anoxia, nitrification becomes inhibited leading to the net accumulation of NH_4^+ which may subsequently lead to phytotoxicity and/or enhanced NH_3 volatilization, while denitrification can lead to the loss of residual soil NO_3^- as N_2O/N_2, particularly when labile SOC is present (Senbayram et al., 2012). Under waterlogging, a drop in redox potential can cause the reduction and solubilisation of Fe^{3+} inducing the release of P held on the surfaces of Fe-oxyhydroxides. Ultimately, this can cause a redistribution of nutrients adsorbed on Fe oxides within the soil profile.

The deleterious effect of flooding on plant growth and soil functions appears to be critically dependent on the duration and timing of the event (Glaz and Lingle, 2012; Shao et al., 2013). Typically, little adverse effect is seen if the floodwater dissipates within 2 weeks, however, longer inundation periods may trigger major changes in soil functioning and ecosystem service delivery (Niu et al., 2014). Finally, the size and composition of the soil microbial community, a key driver for soil functioning and soil-based ecosystem services, is strongly affected by water content and temperature (Castro et al., 2010) and, traditionally, alterations in its structure have

been described during flooding, such as a reduction in Gram− bacteria and an increase in Gram+ bacteria (Bossio and Scow, 1998).

Given the increased frequency of extreme flood events, it is important that we gain a better mechanistic understanding of how this affects soils both during and after flooding. The results obtained in this laboratory experiment under controlled conditions, which allow us to assess different scenarios easily, indicate the main alterations that could happen under field conditions. Field experiments dealing with extreme flooding events will benefit from the results obtained here. This will support the design of successful flood-amelioration strategies to offset the negative effects of flooding and will also inform future soil management regimes. As temperature is a key regulator of biochemical reaction rates in soil, we hypothesize that season will be one of the most important factors which determines the outcome of flooding on soil functioning, air quality and soil microbial communities. To evaluate this, we simulated an extreme flood event at 5 °C (winter flood), 15 °C (spring/autumn flood) and 25 °C (summer flood) in a grassland soil with no previous history of flooding. We investigated nutrient dynamics and potential losses, GHGs emissions, NH_3 volatilization, changes in soil microbial communities and biomass production during an extreme flooding event (8 weeks) and after the flood water was removed, during the recovery of these soils (9 weeks of recovery). Unflooded grassland soil at the same temperatures was used as baseline to compare with the flooded ones.

We selected a grassland soil because of its importance not only in the UK but also worldwide, and the services and soil functions that it provides, including its ability to improve soil C sequestration after a conversion from previously degraded soils (Hirsch et al., 2016). We hypothesized that the magnitude of the response will be more evident (a greater loss of soil functioning, a bigger deterioration of air quality, major alterations in the soil microbial communities and higher reductions in biomass production) and that different mechanisms and reactions will be involved at higher temperatures.

2. Materials and methods

2.1. Soil sampling and soil characterization

125 Twenty-four 10 × 10 × 10 cm intact soil blocks of around 1 kg weight with their
126 indigenous vegetation were collected from the top soil (Ah horizon) of a sheep-grazed grassland,
127 dominated by *Lolium perenne* L. located in Abergwyngregyn, North Wales (53º14'21" N,
128 4º00'57" W) in spring 2016. The soil is classified as a Eutric Cambisol (IUSS Working Group
129 WRB, 2015) with a sandy clay loam texture that receives each year 100 kg N ha^{-1}, 20 kg P ha^{-1}
130 and 20 kg K ha^{-1}. The site has a mean annual soil (0-10 cm) temperature of 10 °C (daily mean
131 ranges from −2.5 to 23 °C) and annual rainfall of 1060 mm.

132 A representative soil sample of one kg was collected from the same area, air-dried for one
133 week at 25 °C and sieved (2 mm) to characterize the main physical-chemical properties. The pH
134 (6.0) and the electrical conductivity (< 0.1 dS m^{-1}) were determined in a 1:2.5 (*w*/*v*) soil:distilled
135 water suspension. Fifty ml of 0.5 M $BaCl_2$ were used to extract the exchangeable bases from 5 g
136 of soil, after shaking for 1 h at 20 °C, and the cations (1600 mg Ca kg^{-1}, 120 mg K kg^{-1}, 90 mg
137 Mg kg^{-1}, 30 mg Na kg^{-1}, 22 mg Al kg^{-1}) analysed with a Series 720 ICP-OES (Agilent
138 Technologies Inc., Santa Clara, CA). Total organic carbon (C, 21.0 g kg^{-1}) and nitrogen (N, 1.6
139 g kg^{-1}) in soil were determined using a CHN-2000 analyser (Leco Corp., St Joseph, MI).

140 A 0.5 M K_2SO_4 solution was used to extract mineral N in a ratio 1:5 soil:extractant (*w*/*v*),
141 shaking for 30 min at 150 rev min^{-1} before centrifuging at 8540 *g* for 10 min. Ammonium (1.4 g
142 kg^{-1}) and NO_3^- (14.0 g kg^{-1}) in the extract were determined colorimetrically according to
143 Mulvaney (1996) and Miranda et al. (2001), respectively, using a PowerWave-XS microplate
144 reader (BioTek Instruments Inc., Winooski, VT). Finally, P availability index (10.0 g kg^{-1}) was
145 measured according to the molybdate blue method of Murphy and Riley (1962), after extracting
146 P from the soil (1 h, 200 rev min^{-1}) using a 1:5 (*w*/*v*) soil:0.5 M acetic acid solution.

147

148 *2.2. Experimental design, treatments and phases of the experiment*

149 The twenty-four intact soil blocks were placed at the bottom of transparent containers
150 made of polypropylene (11 × 8 cm base and 27 cm high; Lock & Lock Ltd., Seoul, Republic of
151 Korea) and distributed equally among three identical Fitotron® plant growth chambers (Weiss
152 Technik UK Ltd, Ebbw Vale, UK) with a photoperiod of 16 h d^{-1}, light intensity of 350 µmol m^{-2}

153 s^{-1}, and relative humidity of 70%, each one with a different temperature, 5 °C, 15 °C or 25 °C,
154 for the whole length of the experiment. A Rhizon® sampler (0.15 μm pore size; Rhizosphere
155 Research Products, Wageningen, The Netherlands) was inserted into the middle of each soil block
156 at an angle of 45° and a depth of 5 cm at the beginning of the experiment to recover soil solution
157 throughout the experiment (i.e. to minimize damage to soil structure and indigenous vegetation).
158 This experiment had three distinct phases:
159 (1) Pre-flood phase: During the first 20 d of the experiment, the plant-soil mesocosms were kept
160 field-moist (ca. 75 % of field capacity) weighing them twice per week and watering individually
161 with oligotrophic water collected from the Aber River (53º14'09" N, 4º01'01" W), located near
162 to the field where the plant and soil samples were taken. The concentration of nutrients in the
163 river water was low (3.1 mg C L^{-1}, 0.16 mg NO_3-N L^{-1}, 0.01 mg NH_4-N L^{-1}, 0.04 mg P L^{-1}, pH
164 6.5).
165 (2) Flood-phase: Four mesocosms at each temperature (5 °C, 15 °C and 25 °C) were flooded (F)
166 with 0.9 L of river water while the other four were watered with river water to keep field-moist
167 (C). The three temperatures were designed to simulate winter, spring/autumn and summer
168 flooding temperatures, although the rest of variables were the same (moisture of the growth
169 chambers, photoperiod, light intensity), to assess the effect of the temperature (main objective).
170 The floodwater depth was maintained 10 cm above the soil surface for eight weeks reflecting
171 unprecedented flooding events observed in the general region in 2016. The treatments were called
172 control 5 °C, control 15 °C, control 25 °C, flood 5 °C, flood 15 °C and flood 25 °C. Therefore,
173 six treatments from the combination of the factor temperature (5 °C, 15 °C and 25 °C) and
174 flood/non-flood and four mesocosms per treatment were used in this experiment.
175 (3) Soil recovery phase: The last phase started by carefully removing the floodwater from the
176 containers that were flooded in the previous stage. Non-flooded, field-moist conditions were
177 subsequently maintained for nine weeks in all 24 mesocosms.
178
179 *2.3. Soil chemical indicators*

Soil solution and floodwater (only during the second phase for the flooded mesocosms) were sampled weekly using a Rhizon® sampler and a pipette, respectively. A Model 209 pH meter (Hanna Instruments Ltd., Leighton Buzzard, UK) was used to measure the pH, while a PowerBase-XS microplate reader (BioTek Instruments Inc., Winooski, VT) was used for the colorimetric determination of P (Murphy and Riley, 1962), Fe (Loeppert and Inskeep, 1996), NH_4^+ (Mulvaney, 1996) and NO_3^- (Miranda et al., 2001). The potential losses of these nutrients were calculated from the maximum concentrations measured in the soil solution and floodwater during the flood phase ($C_{release}$, Eqn. 1):

$$C_{\text{release}}\ (\text{mg mesocosm}^{-1}) = [C_{\text{sol}} \times V_{\text{soil}} \times \Theta] + [C_{\text{flood}} \times V_{\text{flood}}] \qquad \text{(Eqn. 1)}$$

where C_{sol} and C_{flood} are the concentration of a nutrient in the soil solution and floodwater respectively, V_{soil} and V_{flood} are the volume of soil (0.7 l) and floodwater (0.9 l) respectively and Θ is the volumetric water content (0.5 $m^3\ m^{-3}$).

2.4. Greenhouse gas emissions and NH_3 losses

Gas samples were taken on a weekly basis for the flood and recovery phases except the week in which the floodwater was removed when three gas samplings were done. Firstly, a lid with rubber septum was used to hermetically seal the containers. At time 0 h and 1 h, the headspace gas was then sampled using a syringe and extracted gas samples placed in pre-evacuated gas-tight glass vials (22 ml). The concentrations of GHG in the vials was measured using a Clarus 500 gas chromatograph equipped with a HS-40 Turbomatrix autoanalyzer (PerkinElmer Inc., Waltham, MA); CH_4 and CO_2 were detected with a flame ionization detector (FIC) connected to a methanizer and N_2O with a ^{63}Ni electron-capture detector. Greenhouse gas fluxes were calculated with the difference of each gas concentration at time 0 and 1 h after correction for temperature and the ratio between chamber volume and soil surface area (Mackenzie et al., 1998).

The linearity of the fluxes was determined in Sánchez-Rodríguez et al. (2018a). Total cumulative fluxes were estimated by multiplying the mean of two successive daily fluxes by the number of hours between these gas samplings and summing that value to the previous cumulative

208 total. The global warming potential (GWP) of the GHGs was estimated in CO_2 equivalents by
209 multiplying the total cumulative fluxes by 34 for CH_4, 1 for CO_2 and 298 for N_2O before summing
210 them (IPCC, 2013).

211 Ammonia volatilization was estimated by trapping evolved NH_3 using headspace acid
212 traps. Briefly, 25 mm diameter glass microfiber filters saturated with 0.15 M H_3PO_4 (one per
213 mesocosm and sampling; Whatman GmbH, Dassel, Germany) were suspended on the underside
214 of the container lids (while GHG sampling). After one hour in contact with the air inside the
215 hermetically closed container, the filters were removed and the filter papers extracted with 1 ml
216 of distilled water (1 h, 200 rev min^{-1}) before colorimetric determination of NH_4^+ in the extract
217 according to the salicylic acid-hypochlorite procedure of Mulvaney (1996). Weekly samplings
218 were done from the beginning of the flooding to the fourth week of soil recovery.

219

220 *2.5. Soil biological indicators*

221 Soil (25 g) was removed from each mesocosm at the beginning and end of the soil
222 recovery phase, sieved to 2 mm and stored at −80 °C. Subsequently, the samples were freeze-
223 dried and phospholipid fatty acid (PLFA) analysis undertaken according to Bartelt-Ryser et al.
224 (2005) with taxonomic groups ascribed to individual PLFAs using the Sherlock® PLFA Method
225 and Tools Package (PLFAD1; Microbial ID Inc., Newark, DE). One hundred and two fatty acids
226 were identified in the soil samples, however, we only present results from the twenty-nine whose
227 concentration was higher than 0.5% of the total PLFAs (and the one used as a biomarker for
228 protozoa which only constituted 0.4% of the total PLFAs), classified per taxonomic group
229 (Bartelt-Ryser et al., 2005; Bedard and Knowles, 1989; Bossio and Scow, 1998; Bowman et al.,
230 1991, 1993; Kieft et al., 1994; Niklaus et al., 2003; Olsson et al., 1999; Paul and Clark, 1996;
231 Ratledge and Wilkinson, 1988; Zelles, 1999):
232 14:0 iso, 15:0 iso, 15:0 anteiso, 15:1 iso ω 6c, 16:0 iso, 17:0 iso, 17:0 anteiso and 17:1 iso ω9c
233 were used for Gram+ bacteria; 16:1 ω 5c, 16:1 ω7c, 16:1 ω9c, 17:1 ω8c, 17:0 cyclo ω7c, 18:1
234 ω5c, 18:1 ω7c, 18:1 ω9c and 19:0 cyclo ω7c were used for Gram− bacteria; 16:0 10 methyl, 17:1
235 ω7c 10 methyl, 18:0 10 methyl and 18:1 ω7c 10 methyl for actinomycetes; 15:0 DMA as

biomarker for anaerobic bacteria; 20:4 ω6c for protozoa; 18:2 ω6c for fungi; and 16:1 ω5c as biomarker for putative arbuscular mycorrhizal fungi; 14:0, 15:0, 16:0, 17:0, 18:0 were found but were not assigned to a specific taxonomic group.

At the end of the soil recovery phase, the grass was cut, and dry weight recorded after oven drying (80 °C, 48 h) to establish how the different treatments altered plant productivity.

2.6. Statistical analysis

Analysis of variance (ANOVA) with six treatments (three temperatures, 5, 15 and 25 °C, with and without flood) and four replications per treatment was used to determine differences in potential losses of nutrients, cumulative GHG fluxes, GWP, cumulative apparent NH_3 and plant biomass at the end of the experiment, and microbial biomass and taxonomic groups (PLFAs) after the flood phase and after the soil recovery phase. When significant differences were found ($p < 0.05$), Tukey´s HSD *post hoc* was used to separate means of the six treatments. Potential losses of Fe and NO_3^-, cumulative CH_4 and N_2O fluxes, and plant biomass were log10-transformed, and putative arbuscular mycorrhiza was squared-transformed, to meet the requirements for ANOVA. Principal component analysis (PCA) based on a data correlation matrix with principal components (PCs) was developed at the end of the flood phase and after soil recovery to evaluate alterations in soil microbial communities (PLFAs, taxonomic groups).

All the statistical analyses were performed in the statistical package SPSS software v22.0 (IBM Inc., Armonk, NY) except for the PCA, which was done in R' (R Core Team, 2003) with the *Vegan* package (Oksanen et al., 2018) to include additional variables (pH, P, Fe, NH_4^+, NO_3^-, GHG fluxes and apparent NH_3) as environmental factors based on their correlations with the different taxonomic groups. Significance was evaluated using the permutation test (Bonferroni´s correction).

3. Results

3.1. pH, soil nutrient dynamics and potential losses

263 The pH in soil solution fluctuated (range of 6.5-8.5) for the six treatments over the course
264 of the experiment (Fig. 1a). The lowest values were measured for the containers at 5 °C while the
265 highest pHs were measured in the soil solution of the unflooded mesocosms at 25 °C except in
266 the last three samplings for the flooded containers at 25 °C. The pH in the floodwater increased
267 with temperature (Fig. 1b).

268 The concentration of P in the soil solution was also variable throughout the experiment
269 but a general trend in which the highest concentrations were measured for the mesocosms with
270 the lowest temperatures (in 13 of 17 samplings) was observed (Fig. 1c). The trend was the
271 opposite for the P released into the floodwater, with the lowest concentration of P found in the
272 floodwater of the flooded mesocosms at 5 °C (Fig. 1d). Iron in the soil solution was much greater
273 in the flooded treatments than in the control ones, peaking at around 15 mg Fe L^{-1} one week after
274 the flood started for the containers at 25 °C and the last week of the flooding phase for the
275 containers at 15 °C, and around 6 mg Fe L^{-1} in the last week of the flood phase for the containers
276 at 5 °C (Fig. 1e). The concentration of Fe in the soil solution of the unflooded treatments was
277 negligible in most occasions and below 3 mg Fe L^{-1} in the rest. As for P, the release of Fe into
278 the floodwater was positively related to temperature, except in the last two weeks of the flood
279 phase when the highest concentrations of Fe were found in the mesocosms at 15 °C (Fig. 1f).

280 The time course of NH_4^+ in the soil solution and floodwater followed a similar pattern as
281 described for Fe, with negligible concentrations in the pre-flood phase but which rapidly increased
282 and peaked as a function of the temperature (25 > 15 > 5 °C; Figs. 2ab). A gradual reduction in
283 soil solution NH_4^+ concentration was seen when the floodwater was removed in all treatments. In
284 contrast, the initial concentrations of NO_3^- in soil solution were between 6 and 30 mg N L^{-1} but
285 then, during the flood phase, they remained low except for the unflooded mesocosms at 5 °C, in
286 which these concentrations were higher than for the rest of the unflooded mesocosms (but always
287 below 12 mg N L^{-1}; Fig. 2c). These concentrations were lower than 4 mg N L^{-1} in the floodwater
288 of the three treatments (Fig. 2d). However, NO_3^- in the soil solution of the flooded containers in
289 the soil recovery phase reached values of nearly 60 mg N L^{-1} at 25 °C and 12 mg N L^{-1} at 15 °C.

290 Table 1 displays the potential losses of nutrients from soil for the six treatments during
291 flooding. In general, the combination of flooding × higher temperatures significantly ($p < 0.001$)
292 increased the potential losses (kg ha^{-1}) of P (between 5.0 ± 0.2 and 9.6 ± 0.7), Fe (between 3.9 ±
293 0.6 and 13.7 ± 1.3) and NH_4^+ (between 2.4 ± 0.4 and 17.3 ± 1.0) in comparison with the unflooded
294 mesocosms (1.9 kg ha^{-1} for P and lower than 0.5 kg ha^{-1} for Fe and NH_4^+, Table 1).
295
296 *3.2. GHG fluxes and apparent NH_3 volatilization*
297 Daily GHG fluxes and apparent NH_3 volatilization are shown in Figure 3. Significant CH_4
298 emissions were only detected during the flood phase and the day after the floodwater was removed
299 for the 15 and 25 °C flooding treatments only (Fig. 3a). These daily emissions were greater and
300 more prolonged at 25 °C than at 15 °C, reaching up to 90 and 25 mg C m^{-2} h^{-1}, respectively. In
301 the case of CO_2, daily fluxes were higher in the flooded mesocosms than in the control ones,
302 except for the first gas sampling period (Fig. 3b). Above-background N_2O fluxes were only
303 detected during the soil recovery phase for two treatments, peaking at 3.2 mg N m^{-2} h^{-1} for the
304 flooded containers at 25 °C and around 1 mg N m^{-2} h^{-1} for those held at 15 °C, one week and four
305 weeks after flood removal, respectively (Fig. 3c). Finally, NH_3 emissions were concentrated in
306 the flood phase and only occurred in the flooded mesocosms at the two highest temperatures,
307 reaching up to 0.75 mg N m^{-2} h^{-1} at 25 °C and 0.15 mg N m^{-2} h^{-1} at 15 °C (Fig. 3d).
308 The control treatment at 25 °C was the only treatment that acted as a sink for cumulative
309 CH_4 and N_2O fluxes (Table 2). The highest cumulative fluxes ($p < 0.001$) were produced in the
310 flooded containers at 25 °C, followed by the ones at 15 °C, and then the rest of combinations.
311 Negative cumulative CO_2 fluxes were calculated for the unflooded mesocosms at 15 and 25 °C.
312 GWP was significantly higher ($p < 0.001$) for the flooded mesocosms at 25 °C in comparison
313 with the rest of the treatments (Table 2), with CH_4 accounting for 82% of the GWP for this
314 treatment. Finally, cumulative N losses due to apparent NH_3 volatilization were significantly
315 higher ($p < 0.001$) for the flooded mesocosms at 25 °C, followed by flooded mesocosms at 15 °C,
316 and lastly, by the rest of mesocosms.
317

318 *3.3. Soil microbial communities*

319 Flooding at different temperatures significantly altered the size and structure of the soil
320 microbial communities, some of which persisted through to the end of the soil recovery phase.
321 Soil microbial biomass was significantly reduced ($p < 0.001$) for the combination flood × 25 °C
322 to 58.8% of the equivalent unflooded treatment at the end of the flooding, and to 66.7% after soil
323 recovery (Table 3). Gram+ bacteria (%) were increased ($p < 0.001$) due to the effect of flooding
324 and higher temperature after the floodwater phase, while a similar effect occurred for Gram−
325 bacteria after the soil recovery in the flooded mesocosms ($p < 0.001$ for both). Actinomycetes
326 were negatively affected ($p = 0.002$ and $p < 0.001$) by temperature for the flooded containers,
327 especially in the second sampling. Flooding produced the lowest (at 5 °C) and the highest (at 25
328 °C) percentage of protozoa after soil recovery ($p = 0.032$). The proportion of putative arbuscular
329 mycorrhiza fungi and fungi (%) both decreased with increasing temperature but mainly because
330 of the combination flooding × higher temperatures. Fungi after soil recovery (Table 3) was an
331 exception to this where the 25 °C flooded mesocosms were found to have the highest percentage
332 of fungi.

333 The PCA for the different taxonomic groups (PLFAs) and their relationships with the
334 environmental variables is shown in Fig. 4a. The separation of treatments after the flood phase
335 and soil recovery can be seen in Fig. 4b and Fig. 4c, respectively. The first PC, accounting for
336 55% of the total variance, was related with opposing shifts in Gram− bacteria and actinomycetes.
337 The second PC explained 30% of the total variance and was mainly related to the abundance of
338 Gram+ bacteria. The differences between soil microbial communities were more evident at higher
339 temperatures and in the first sampling (Figs. 4bc), with a similar microbial structure for the lowest
340 temperature in flooded and unflooded mesocosms after soil recovery (Fig. 4c).

341 On one hand, the flooded mesocosms, in the order 25 °C > 15 °C > 5 °C, were more
342 related to higher pH, solution nutrient concentration (except for NO_3^-), higher GHG fluxes (CH_4
343 after the flood phase and N_2O after soil recovery), Gram+ bacteria after the flood phase and
344 Gram− bacteria after soil recovery. On the other hand, the unflooded containers, in the order 25
345 °C > 15 °C > 5 °C, were more related to higher NO_3^- in soil solution, actinomycetes and putative

arbuscular mycorrhiza contents, with this effect clearer after the flood phase (Fig. 4b) than after the soil recovery (Fig. 4c). Some significant correlations between the PCs and the environmental variables were found: pH (r = 0.59, p = 0.009), Fe (r = 0.75, p = 0.009), NH_4^+ (r = 0.59, p = 0.018), CH_4 (r = 0.71, p = 0.009), CO_2 (r = 0.65, p = 0.009) and apparent NH_3 (r = 0.75, p = 0.009).

3.4. Plant biomass

The plants growing in the flooded mesocosms at 15 and 25 °C started showing chlorosis two weeks after the floodwater was added and even necrosis in some of the leaves. Damage was greatest at the highest temperature, but no visual differences were observed between the plants growing in the control and flooded containers at 5 °C. The vegetation in the flooded containers at 25 °C completely died after 3-4 weeks of flooding. Overall, flooding limited plant dry weight (kg m^{-2}) at 5 °C (0.82 ± 0.09 vs 0.68 ± 0.10), 15 °C (1.49 ± 0.03 vs 0.75 ± 0.44) and 25 °C (2.68 ± 0.15 vs 0.12 ± 0.09), although the difference only proved significant at 25°C (Fig. 5).

4. Discussion

4.1. Biomass production, element cycling and water quality

Our study showed a clear interactive effect of flooding and temperature on soil functions or processes within intact grassland mesocosms. It is clear that temperature is a dominant factor regulating biomass production and soil functions under an extreme flood event: a biomass reduction of 95% relative to the controls was observed at 25 °C. This mirrors the devastating effects that spring and summer floods have been shown to have on agricultural production (loss of crop quality and yield), even when the length of the event is short (3-4 weeks) (Klaus et al., 2016; Posthumus et al., 2009).

Flooding induced rapid changes in many soil chemical quality indicators, with the effects seen faster at elevated temperatures (25 > 15 > 5 °C). Although P and NO_3^- in soil solution were in general lower at the end of the experiment than at the beginning, the majority of these indicators returned to their pre-flood values after a few weeks of soil recovery demonstrating the resilience

374 of this grassland soil which has no previous history of inundation (Sánchez-Rodríguez et al.,
375 2017). However, the extreme events induced a release of nutrients (P, Fe and N in the form of
376 NH_4^+) from the system and a significant increase of their potential losses, especially at high
377 temperatures. Nutrient losses could pollute new areas where the floodwater is discharged,
378 contribute to the eutrophication of adjacent water bodies or even produce toxicity due to soil
379 accumulation of phytotoxic elements (e.g. Fe or Mn; Millaleo et al., 2010). Therefore, an
380 immediate reduction in soil fertility may be expected after an extreme flood event. Although it
381 will depend on the soil, nutrient content and bioavailability it could affect grassland sustainability
382 and resilience under future events. In addition, in a scenario in which the frequency of extreme
383 flood events and mean global temperature are increasing, soil functions and processes such as
384 habitat provision, element cycling and water cycling (water quality) could be damaged to a greater
385 extent if no alleviation measures are implemented.

386 Soil solution pH was highly variable and provided a poor indicator of alterations caused
387 by flooding. A large drop in redox potential and the release of Fe into solution was predicted to
388 induce the release of P held on Fe oxide surfaces. Little evidence for this was seen, however,
389 suggesting that any P released was either immobilized in the microbial biomass, re-sorbed to other
390 mineral surfaces [e.g. $Al(OH)_3$], or was taken up by living plants (at 5 and 15 °C). The loss of P
391 to the floodwater we ascribe to the decomposition and release of P from the above-ground
392 vegetation (Sánchez-Rodríguez et al., 2019).

393 The N cycle suffered significant alterations depending on the temperature of the flood
394 event. As expected, nitrification was limited during the flood phase (Nielsen et al., 1996).
395 Evidence for nitrification was only found for the control treatment at the lowest temperature
396 (really low NO_3^- concentrations in the soil solution and lack of N_2O emissions for the rest of the
397 temperatures). We hypothesize that plant uptake of inorganic N most likely explains their low
398 concentration in the unflooded mesocosms and to a lesser extent for the flooded mesocosms as
399 plants growing in these conditions close their stomata and reduce the uptake of water soluble
400 nutrients as a response (Milroy and Bange, 2013). There was an accumulation of NH_4^+ in the
401 flooded mesocosms (soil solution and floodwater) that we hypothesise could have had two

different origins and contributions depending on the temperature: (1) mineralization of organic matter which increases with temperature (Kirwan and Blum, 2011); and (2) death of plants at higher flood temperatures, reducing the possibility of plant NH_4^+ uptake.

This NH_4^+ accumulation occurred rapidly in the flooded mesocosms at 25 °C (peaking 7 d after flooding for soil solution, and 14 d for the floodwater), and a bit slower for the mesocosms at 15 °C (peaking after three-four weeks of flooding), in comparison with the containers at 5 °C. A considerable decrease in these NH_4^+ concentrations was observed at the two highest temperatures during the flood phase, probably due to NH_3 volatilization as seen by Chen et al. (2015) for prolonged flooded rice crops. After that, a rapid reduction in NH_4^+ concentration in the soil solution of the flooded containers was seen during soil recovery, linked to an increase in NO_3^- and N_2O emissions, higher at higher temperatures, indicating that the nitrifier population was unaffected by flooding. This is in line with Xu et al. (2016) who reported an increase in gene abundance and activity of the nitrifiers with temperature.

4.2. Air quality and global warming potential

The release of CH_4 was seen only during the flood phase and the day the floodwater was removed. We ascribe the latter to the degassing of CH_4 previously trapped in soil pores rather than *de novo* production. Methane production under flooding was clearly enhanced by the temperature and were analogous to those measured by Zhou et al. (2018) for subtropical permanently flooded rice paddy fields in China (up to 900 kg CH_4-C ha^{-1} yr^{-1}). We speculate that the rapid death of roots, particularly at high temperatures, led to the release of labile C into the soil supporting microbial activity and fuelling a rapid lowering of the redox potential below −100 mV and production of CH_4 (Hou et al., 2000). Alternatively, this process could have been driven by the release of lactic acid and ethanol into the soil from live roots under hypoxia (i.e. respiratory C dumping; Jones et al., 2009). The loss of alternative electron acceptors from soil solution (e.g. NO_3^-) alongside the rapid accumulation and stabilization of the end-products (e.g. Fe^{2+}) also suggests a very rapid drop in redox potential at higher temperatures. The rapid cessation of CH_4 production after removal of floodwater and the evidence for the emergence of more superior

alternative electron acceptors (NO_3^-, Fe^{3+}), however, suggests that methanogenic activity was rapidly inhibited or that any CH_4 produced was consumed by methanotrophs.

The daily and cumulative CO_2 fluxes were higher in the mesocosms where the vegetation had a lower photosynthetic activity, under flooding at 25 °C (no plants survived), and the lowest CO_2 fluxes were measured for the unflooded mesocosms at 15 and 25 °C, which had the highest fixation of C and biomass production. This is the opposite to that observed in similar experiments without vegetation (Sánchez-Rodríguez et al., 2018b), but agrees with Lewis et al. (2014) for fluxes measured in vegetated coastal wetlands. Overall, the total amount of gaseous C loss (CO_2 + CH_4) from the most impacted treatment (flood, 25 °C) was 1.2 g C kg^{-1} over the 49 d experimental period. Probably, this high C flux is in part due to the large amount of decaying plant material which is senescing and being broken down. It would be interesting to compare these values with the results obtained in future field experiments under similar temperatures (winter/spring-autumn/summer flood events) to quantify how extreme flood events could affect long-term C storage.

In our experiment, N_2O was only produced in significant quantities in the recovery phase. At the start of the experiment the soil solution NO_3^- concentrations were low and it is highly likely that most of this was fully denitrified to N_2 shortly after flooding (Reddy and Patrick Jr., 1975). It is well established, however, that N_2O production is optimal at water filled pore space values of between 60-70% which would have occurred after flood water removal (Bateman and Baggs, 2005). This soil is known to have an intrinsically high net nitrification rate (ca. 0.42 mg N kg^{-1} d^{-1}; Jones et al., 2004), and therefore N_2O may have been produced via both nitrification and/or denitrification as the NH_4^+ accumulated during flooding (ca. 5 mg N kg^{-1}) was subsequently converted to NO_3^-. At 25 °C, the N_2O emission window lasted ca. 22 d with a mean N_2O flux of 0.51 mg N_2O-N kg^{-1} d^{-1} (i.e. 11.2 mg N_2O-N kg^{-1}). This indicates that N_2O was also produced from *de novo* mineralization of soil organic N (SON) after floodwater removal, presumably in response to an accelerated turnover of the soil microbial community and the removal of O_2 limitation on SON breakdown (pool size 1600 mg N kg^{-1}) after flood water removal. Our measured fluxes (equivalent to 6 and 14 kg N_2O-N ha^{-1} at 15 and 25 °C, respectively) were

458 considerably higher than those measured by Zhou et al. (2018) in flooded rice (6 kg N_2O-N ha^{-1}
459 yr^{-1}), and than those calculated in field experiments with winter wheat fertilized with 190 kg N
460 ha^{-1} as digestate (0.7 kg N_2O-N ha^{-1}) on the same soil (Sánchez-Rodríguez et al., 2018a).

461 Field experiments monitoring extreme flood events are necessary to check if extreme
462 flood events can cause similar or higher GHG emissions than those produced from agricultural
463 management events (e.g. fertilizer addition, tillage). However, monitoring emissions during real
464 extreme flood events remains highly challenging as they are notoriously difficult to predict, it is
465 problematic to logistically deploy GHG equipment, and they frequently lack a counterfactual
466 control treatment. In view of the potential GHG emissions reported here under flooding and the
467 large land surfaces that are affected by these extreme floods (Klaus et al., 2016; Met Office, 2014),
468 there is an urgent need to produce more accurate GHG emission estimates from these events. This
469 will be useful to help explain differences between top-down and bottom-up GHG emission
470 calculations as well as seasonal patterns in observed atmospheric concentrations (Ganesan et al.,
471 2015), and to aid the design of more sustainable GHG mitigation strategies. It should also be
472 considered that the gaseous loss of NH_3 in particular both during and after flooding not only
473 affects soil functioning but also negatively impacts on air quality and should be considered further
474 (Galloway et al., 2003).

475 Finally, these losses of nutrients via gaseous emissions also alter soil functions such as
476 habitat provision, element, water and organic matter cycling that are essential for essential soil-
477 based ecosystem services, i.e. biomass production, biodiversity conservation, water quality and
478 supply and climate regulation. Consequently, agricultural management and practices in locations
479 where there is a high risk of flooding (historically or in recent years) should be more focused on
480 maintaining these soil functions with fertilizer and organic matter applications, particularly after
481 extreme flood events. If possible, they should improve the drainage and the water evacuation
482 facilities (e.g. water pumping stations) to minimize the time that the floodwater remains on the
483 land.

484

485 *4.3. Habitat provision for soil organisms: Soil microbial communities and their relationship with*
486 *environmental factors*

487 As used in previous studies, PLFA analysis was used to provide a broad scale assessment
488 of changes in soil microbial communities induced by flooding (Bossio and Scow, 1998; Liao et
489 al., 2018; Pan et al., 2016). Although PLFA groups cannot be quantitatively compared against
490 each other (e.g. fungal biomass vs Gram+ biomass), they do provide a relative indication of how
491 experimental treatment affects each group. Overall, extreme flooding caused a reduction in total
492 microbial biomass, particularly at higher temperatures. During flooding it was expected that the
493 microbial biomass would increase at 25 °C in response to the death of the vegetation and a large
494 input of labile C to the soil. However, our results strongly suggest that maintaining live roots and
495 an active rhizosphere is more important for preserving the microbial community. This is
496 particularly true for obligate biotrophs such as arbuscular mycorrhizal fungi (AM fungi). Poor
497 plant growth in the recovery phase might also explain why the microbial biomass and AM fungal
498 biomass did not recover in the 25 °C flooded treatment, even when O_2 was restored to the system.

499 Flooding also induced a very large reduction in total fungal biomass relative to other
500 taxonomic groups (by >50% at 15 and 25 °C). With a few exceptions, these fungi are almost all
501 obligate aerobes (Tonouchi, 2009), consequently it is not surprising that their loss is induced by
502 long-term flooding and anoxia. This sensitivity of fungi to waterlogging suggests that this metric
503 may provide a good indicator of flood stress within the microbial community.

504 Gram+ bacteria are typically considered to be more resistant to stress (Guckert et al.,
505 1985) and were shown to increase in response to flooding in a previous study (Bossio and Scow,
506 1998). We found a similar effect during flooding, however, this effect did not persist after the soil
507 recovery phase. In contrast, the actinomycetes, a filamentous subset of the Gram+ bacteria, were
508 found to decrease in response to flooding. Similar to fungi, we ascribe this response to their
509 obligate aerobic nature. Gram− bacteria are generally considered to be fast growing in comparison
510 to Gram+ bacteria. It is possible that the small increase in their population upon flood removal
511 was due to them filling the niche space left by fungi in the soil.

These results highlight the essential role of vegetation for maintaining soil microbial communities in this grassland soil and the importance in providing soil-based ecosystem services (biomass production, biodiversity conservation, water quality and supply and climate regulation). The use of flood-resistant plant species would help maintain the delivery of these ecosystem services in flood prone areas. Lastly, the persistent alterations in microbial community seen even after flood recovery also indicate that soil biological indicators are more sensitive than most routine chemical indicators.

5. Conclusions

In this study, we show that extreme flood events negatively impact upon soil functioning and soil-based ecosystem services, and water quality of an intact grassland soil, with the damage being more severe at higher temperatures. Clear alterations in element cycling and dynamics, biomass production and GHG emissions were produced in the short-term and biological alterations (biological population regulation, microbial biomass and structure of soil microbial communities) in the mid-term. This mesocosm experiment provides clear evidence that ecosystem responses to extreme weather events are highly dependent on temperature. It is predicted that extreme events of different types are likely to become more frequent in the future and consequently, extreme events may occur in close succession (e.g. flood followed by drought). Further work, including mechanistic (simulating conditions of the different seasons) and field (different seasons) experiments, is therefore required to determine how flooding alters the resilience of grasslands to future extreme weather events.

Acknowledgments

This work was supported by the Project ‘Legacy effects of the extreme flood events on soil quality and ecosystem functioning’, NERC Grant Reference NE/M005143/1, by the UK Department for Environment, Food and Rural Affairs (DEFRA) project LM0316, by the UK Natural Environment Research Council (NE/I012303/1) and the Sêr Cymru LCEE-NRN project, Climate-Smart Grass. Sánchez-Rodríguez also acknowledges funding support by the ‘Fundación

Ramón Areces' for his postdoctoral scholarship "Beca para ampliación de estudios en el extranjero en materia de Ciencias de la Vida y de la Materia" and the contract "Juan de la Cierva-Incorporación (IJCI-2016-27388)" of the Spanish Ministry of Science, Innovation and Universities.

References

Alongi, D.M., de Carvalho, N.A., Amaral, A.L., da Costa, A., Trott, L., Tirendi, F., 2012. Uncoupled Surface and below-ground soil respiration in mangroves: implications for estimates of dissolved inorganic carbon export. Biogeochemistry 109, 151–162.

Bartelt-Ryser, J., Joshi, J., Schmid, B., Brandl, H., Balser, T., 2005. Soil feedbacks of plant diversity on soil microbial communities and subsequent plant growth. Perspectives in Plant Ecology, Evolution and Systematics 7, 27–49.

Bateman, E.J., Baggs, E.M., 2005. Contributions of nitrification and denitrification to N2O emissions from soils at different water-filled pore space. Biology and Fertility of Soils 41, 379–388.

Bedard, C., Knowles, R., 1989. Physiology, biochemistry, and specific inhibitors of CH_4, NH_4^+, and CO oxidation by methanotrophs and nitrifiers. Microbiology Reviews 53, 68–84.

Blagodatsky, S.A., Heinemeyer, O., Richter, J., 2000. Estimating the active and total soil microbial biomass by kinetic respiration analysis. Biology and Fertility of Soils 32, 73–81.Bossio, D.A., Scow, K.M., 1998. Impacts of carbon and flooding on soil microbial communities: phospholipid fatty acid profiles and substrate utilization patterns. Microbial Ecology 35, 265–278.

Bowman, J.P., Skerratt, J.H., Nichols, P.D., Sly, L.I., 1991. Phospholipid fatty-acid and lipopolysaccharide fatty-acid signature lipids in methane-utilizing bacteria. FEMS Microbiology Ecology 85, 15–22.

Bowman, J.P., Sly, L.I., Nichols, P.D., Hayward, A.C., 1993. Revised taxonomy of the methanotrophs: Description of *Methylobacter* gen. nov., emendation of *Methylococcus*, validation of *Methylosinu*s and *Methylocystis* species, and a proposal that the family

568 *Methylococcaceae* includes only the Group I methanotrophs. International Journal of
569 Systematic Bacteriology 43, 735–753.
570 Bünemann, E.K., Bongiorno, G., Bai, Z., Creamer, R.E., de Deyn, G., de Goede R., Fleskens, L.,
571 Geissen, V., Kuyper, T.W., Mäder, P., Pulleman, M., Sukkel, W., van Groenigen, J.W.,
572 Brussaard, L., 2018. Soil quality – A critical review. Soil Biology and Biochemistry 120,
573 105–125.
574 Castro, H.F., Classen, A.T., Austin, E.E., Norby, R.J., Schadt, C.W., 2010. Soil Microbial
575 Community Responses to Multiple Experimental Climate Change Drivers. Applied and
576 Environmental Microbiology 76, 999–1007.
577 Chen, A., Lei, B., Hu, W., Lu, Y., Mao, Y., Duan, Z., Shi, Z., 2015. Characteristics of ammonia
578 volatilization on rice grown under different nitrogen application rates and its quantitative
579 predictions in Erhai Lake Watershed, China. Nutrient Cycling in Agroecosystems 101,
580 139–152.
581 Das, K.K., Panda, D., Sarkar, R.K., Reddy, J.N., Ismail, A.M., 2009. Submergence tolerance in
582 relation to variable floodwater conditions in rice. Environmental and Experimental Botany
583 66, 425–434.
584 Ganesan, A. L., Manning, A. J., Grant, A., Young, D., Oram, D. E., Sturges, W. T., Moncrieff, J.
585 B., O'Doherty, S., 2015. Quantifying methane and nitrous oxide emissions from the UK
586 and Ireland using a national-scale monitoring network. Atmospheric Chemistry and
587 Physics 15, 6393–6406.
588 Galloway, J. N., Aber, J. D., Erisman, J. W., Seitzinger, S. P., Howarth, R. W., Cowling, E. B.,
589 Cosby, B.J., 2003. The nitrogen cascade. Bioscience 53, 341–356.
590 Glaz, B., Lingle, S.E., 2012. Flood duration and time of flood onset effects on recently planted
591 sugarcane. Agronomy Journal 104, 575–583.
592 Guckert, J.B., Antworth, C.P., Nichols, P.D., White, D.C., 1985. Phospholipid, ester-linked fatty
593 acid profiles as reproducible assays for changes in prokaryotic community structure of
594 estuarine sediments. FEMS Microbiology Ecology 1, 147–158.

595 Hirsch, P.R., Jhurreea, D., Williams, J.K., Murray, P.J., Scott, T., Misselbrook, T.H., Goulding,
596 K.W.T., Clark, I.M., 2017. Soil resilience and recovery: rapid community responses to
597 management changes. Plant and Soil 4, 283–297.
598 Hou, A.X., Chen, G.X., Wang, Z.P., Van Cleemput, O., Patrick Jr., W.H., 2000. Methane and
599 nitrous oxide emissions from a rice field in relation to soil redox and microbiological
600 processes. Soil Science Society of America Journal 64, 2180–2186.
601 IPCC, 2013. Climate Change 2013: The Physical Science Basis. Contribution of Working Group
602 I to the Fifth Assessment Report of the Intergovernmental Panel on Climate Change.
603 Stocker, T.F., Qin, D., Plattner, G.K., Tignor, M., Allen, S.K., Boschung, J., Nauels, A.,
604 Xia, Y., Bex, V., Midgley, P.M. (Eds.). Cambridge University Press, Cambridge, United
605 Kingdom and New York, NY, USA, 1535 pp.
606 IPCC, 2014. Managing the risks of extreme events and disasters to advance climate change
607 adaptation. In: Field, C.B., Barros, V., Stocker, T.F., Qin, D., Dokken, D.J., Ebi, K.L.,
608 Mastrandrea, M.D., Mach, K.J., Plattner, G.K., Allen, S.K., Tignor, M., Midgley, P.M.
609 (Eds.), A Special Report of Working Groups I and II of the Intergovernmental Panel on
610 Climate Change. Cambridge university Press, Cambridge, UK, and New York, NY, USA
611 (p. 582).
612 IUSS Working Group WRB, 2015. World Reference Base for Soil Resources 2014, update 2015.
613 International soil classification system for naming soils and creating legends for soil maps.
614 World Soil Resources Reports No. 106. FAO, Rome.
615 Jones, D.L., Nguyen, C., Finlay, R.D., 2009. Carbon flow in the rhizosphere: carbon trading at
616 the soil–root interface. Plant and Soil 321, 5–33.
617 Jones, D.L., Shannon, D., Murphy, D.V., Farrar, J., 2004. Role of dissolved organic nitrogen
618 (DON) in soil N cycling in grassland soils. Soil Biology and Biochemistry 36, 749–756.
619 Kieft, T.L., Ringelberg, D.B., White, D.C., 1994. Changes in ester linked phospholipid fatty acid
620 profiles of subsurface bacteria during starvation and desiccation in a porous medium.
621 Applied and Environmental Microbiology 60, 3292–3299.

622 Kirwan, M.L., Blum, L.K., 2011. Enhanced decomposition offsets enhanced productivity and soil
623 carbon accumulation in coastal wetlands responding to climate change. Biogeosciences 8,
624 987–993.
625 Klaus, S., Kreibich, H., Merz, B., Kuhlmann, B., Schröter, K., 2016. Environmental Earth
626 Sciences 75: 1289.
627 Lewis, D.B., Brown, J.A., Jimenes, K.L., Effects of flooding and warming on soil organic matter
628 mineralization in *Avicennia germinans* mangrove forests and *Juncus roemerianus* salt
629 marshes. Estuarine, Coastal and Shelf Science 139, 11–19.
630 Liao, H.K., Chapman, S.J., Li, Y.Y., Yao, H.Y., 2018. Dynamics of microbial biomass and
631 community composition after short-term water status change in Chinese paddy soils.
632 Environmental Science and Pollution Research 25, 2932-2941.
633 Loeppert, R.H. Inskeep, W.P., 1996. Iron. In: Sparks DL (Ed.), Methods of Soil Analysis. Part 3.
634 Chemical Methods. ASA/SSSA, Madison, WI, pp. 639–664.
635 Mackenzie, A.F., Fan, M.S., Cadrin, F., 1998. Nitrous oxide emission in three years as affected
636 by tillage, corn-soybean-alfalfa rotations, and nitrogen fertilization. Journal of
637 Environmental Quality 27, 698–703.
638 Met Office, 2014. The Recent Storms and Floods in the UK. Available at:
639 http://nora.nerc.ac.uk/id/eprint/505192/1/N505192CR.pdf
640 Millaleo, R., Reyes-Díaz, M., Ivanov, A.G., Mora, M.L., Alberdi, M., 2010. Manganese as
641 essential and toxic element for plants: transport, accumulation and resistance mechanisms.
642 Journal of Soil Science and Plant Nutrition 10, 476–494.
643 Miller, W.D., Neubauer, S.C., Anderson, I.C., 2001. Effects of sea level induced disturbances on
644 high salt marsh metabolism. Estuaries 24, 357–367.
645 Milroy, S.P., Bange, M.P., 2013. Reduction in radiation use efficiency of cotton (*Gossypium*
646 *hirsutum* L.) under repeated transient waterlogging in the field. Field Crops Research 140,
647 51–58.

Miranda, K.M, Espey, M.G., Wink, D.A., 2001. A rapid simple spectrophotometric method for simultaneous detection of nitrate and nitrite. Nitric Oxide: Biology and Chemistry 5, 62–71.

Morris, J., Brewin, P., 2014. The impact of seasonal flooding on agriculture: the spring 2012 floods in Somerset, England. Journal of Flood Risk Management 7, 128–140.

Mulvaney, R.L., 1996. Nitrogen - inorganic forms. In: Sparks, D.L. (Ed.), Methods of Soil Analysis. Part 3. Chemical Methods. Soil Science Society of America, Madison, WI, pp. 1123–1184.

Murphy, J., Riley, J.P., 1962. A modified single solution method for the determination of phosphate in natural waters. Analytica Chimica Acta 27, 31–36.

Nielsen, T.H., Nielsen, L.P., Revsbech, N.P., 1996. Nitrification and coupled nitrification-denitrification associated with a soil-manure interface. Soil Science Society of America Journal 60, 1829–1840.

Niklaus, P.A., Alphei, J., Ebersberger, D., Kampichler, D., Kandeler, E., Tscherko, D., 2003. Six years of in situ CO_2 enrichment evoke changes in soil structure and soil biota of nutrient-poor grassland. Global Change Biology 9, 585–600.

Niu, S., Luo, Y., Li, D., Cao, S., Xia, J., Smith, M.D., 2014. Plant growth and mortality under climatic extremes: an overview. Environmental and Experimental Botany 98, 13–19.

Oksanen, J., Blanchet, F.G., Friendly, M., Kindt, R., Legendre, P., McGlinn, D., Minchin, P.R., O'Hara, R.B., Simpson, G.L., Solymos, P., Henry, M., Stevens, H., Szoecs, E., Wagner, H., 2018. Vegan: Community Ecology Package. R package version 2.5-2. https://CRAN.R-project.org/package=vegan

Olsson, P.A., Thingstrup, I., Jakobsen, I., Baath, F., 1999. Estimation of the biomass of arbuscular mycorrhizal fungi in a linseed field. Soil Biology and Biochemistry 31, 1879–1887.

Osanai, Y., Tissue, D.T., Bange, M.P., Braunack, M.V., Anderson, I.C., Singh, B.K., 2017. Interactive effects of elevated CO_2, temperature and extreme weather events on soil nitrogen and cotton production under future climate regimes. Agriculture, Ecosystems and Environment 246, 343–353.

676 Pan, F.X., Li, Y.Y., Chapman, S.J., Yao, H.Y., 2016. Effect of rice straw application on microbial
677 community and activity in paddy soil under different water status. Environmental Science
678 and Pollution Research 23, 5941–5948.
679 Paul, E.A., Clark, F.E., 1996. Soil Microbiology and Biochemistry. Academic Press, San Diego,
680 CA.
681 Posthumus, H., Morris, J., Hess, T.M., Neville, D., Phillips, E., Baylis, A., 2009. Impacts of the
682 summer 2007 floods on agriculture in England. Journal of Flood Risk Management 2, 182–
683 189.
684 R Core Team, 2013. R: A language and environment for statistical computing. R Foundation for
685 Statistical Computing, Vienna, Austria. URL http://www.R-project.org/.
686 Ratledge, C., Wilkinson, S.G., 1988. Microbial Lipids. Academic Press, London.
687 Reddy, K.R., Patrick Jr, W.H., 1975. Effect of alternate aerobic and anaerobic conditions on redox
688 potential, organic matter decomposition and nitrogen loss in a flooded soil. Soil Biology
689 and Biochemistry 7, 87–94.
690 Romanescu, G., Stoleriu, C.C., 2017. Exceptional floods in the Prust basin, Romania, in the
691 context of heavy rains in the summer of 2010. Natural Hazards and Earth Systems Sciences
692 17, 381–396.
693 Sánchez-Rodríguez, A.R., Hill, P.W., Chadwick, D.R., Jones, D.L., 2017. Crop residues
694 exacerbate the negative effects of extreme flooding on soil quality. Biology and Fertility of
695 Soils 53, 751–765.
696 Sánchez-Rodríguez, A.R., Hill, P.W., Chadwick, D.R., Jones, D.L., 2019. Typology of extreme
697 flood event leads to differential impacts on soil quality. Soil Biology and Biochemistry
698 129, 153–168.
699 Sánchez-Rodríguez, A.R., Carswell, A.M., Shaw, R., Hunt, J., Saunders, K., Cotton, J., Chadwick
700 D.R., Jones, D.L., Misselbrook, T.H., 2018a. Advanced Processing of Food Waste Based
701 Digestate for Mitigating Nitrogen Losses in a Winter Wheat Crop. Frontiers in Sustainable
702 Food Systems 2:35.

703 Sánchez-Rodríguez, A.R., Chadwick, D.R., Tatton, G.S., Hill, P.W., Jones DL, 2018b.
704 Comparative effects of prolonged freshwater and saline flooding on nitrogen cycling in an
705 agricultural soil. Applied Soil Ecology 125, 56–70.
706 Senbayram, M., Chen, R., Budai, A., Bakken, L., Dittert, K., 2012. N_2O emission and the
707 $N_2O/(N_2O+N_2)$ product ratio of denitrification as controlled by available carbon substrates
708 and nitrate concentrations. Agriculture, Ecosystems and Environment 147, 4–12.
709 Shao, G.C., Lan, J.J., Yu, S.E., Liu, N., Guo, R.Q., She, D.L., 2013. Photosynthesis and growth
710 of winter wheat in response to waterlogging at different growth stages. Photosynthetica 51,
711 429–437.
712 Slater, L.J., Villarini, G., 2016. Recent trends in US flood risk. Geophysical Research Letters 43,
713 12428–12436.
714 Thorne, C., 2014. Geographies of UK Flooding in 2013/4. Geographical Journal 180, 297–309.
715 Tonouchi, A., 2009. Isolation and characterization of a novel facultative anaerobic filamentous
716 fungus from Japanese rice field Soil. International Journal of Microbiology 2009:571383.
717 Trenberth, K. E., 2011. Changes in precipitation with climate change. Climate Research 47, 123–
718 138.
719 Xu, X., Ran, Y., Li, Y., Zhang, Q., Liu, Y., Pan, H., Guan, X., Li, J., Shi, J., Dong, Li, Li, Z., Di,
720 H., Xu, J., 2016. Warmer and drier conditions alter the nitrifier and denitrifier communities
721 and reduce N_2O emissions in fertilized vegetable soils. Agriculture, Ecosystems and
722 Environment 231, 133–142.
723 Zelles, L., 1999. Fatty acids patterns of phospholipids and lipopolysaccharides in the
724 characterization of microbial communities in soil: a review. Biology and Fertility of Soils
725 29, 111–129.
726 Zhou, M., Wang, X., Wang, Y., Zhu, B., 2018. A three-year experiment of annual methane and
727 nitrous oxide emissions from the subtropical permanently flooded rice paddy fields of
728 China: Emission factor, temperature sensitivity and fertilizer nitrogen effect. Agricultural
729 and Forest Meteorology 250–251, 299–307.
730

731 **Figure captions**

732 **Fig. 1** Time course (mean value and standard error) of pH, P and Fe in soil solution and
733 floodwater for the different treatments. 5C: unflooded mesocosms at 5 °C; 15C:
734 unflooded mesocosms at 15 °C; 25C: unflooded mesocosms at 25 °C; 5F: flooded
735 mesocosms at 5 °C; 15F: flooded mesocosms at 15 °C; 25F: flooded mesocosms at 25
736 °C. Four replicates per treatment.

737 **Fig. 2** Time course (mean value and standard error) of NH_4^+ and NO_3^- in soil solution and
738 floodwater for the different treatments. 5C: unflooded mesocosms at 5 °C; 15C:
739 unflooded mesocosms at 15 °C; 25C: unflooded mesocosms at 25 °C; 5F: flooded
740 mesocosms at 5 °C; 15F: flooded mesocosms at 15 °C; 25F: flooded mesocosms at 25
741 °C. Four replicates per treatment.

742 **Fig. 3** Daily CH_4, CO_2 and N_2O fluxes and apparent NH_3 volatilization (mean value and
743 standard error). 5C: unflooded mesocosms at 5 °C; 15C: unflooded mesocosms at 15 °C;
744 25C: unflooded mesocosms at 25 °C; 5F: flooded mesocosms at 5 °C; 15F: flooded
745 mesocosms at 15 °C; 25F: flooded mesocosms at 25 °C. Four replicates per treatment.

746 **Fig. 4** Principal component analysis (PCA) of microbial community PLFAs in response
747 to flooding and temperature. **a** Relationships between taxonomic groups (arrows) that
748 were used for the PCA and environmental variables (small crosses; pH, P, Fe, NH_4^+,
749 NO_3^-, daily CH_4, CO_2 and N_2O fluxes); **b** Treatment separation after the flood phase; and
750 **c** Treatment separation after soil recovery. 5C: unflooded mesocosms at 5 °C; 15C:
751 unflooded mesocosms at 15 °C; 25C: unflooded mesocosms at 25 °C; 5F: flooded
752 mesocosms at 5 °C; 15F: flooded mesocosms at 15 °C; 25F: flooded mesocosms at 25
753 °C. Four replicates per treatment.

754 **Fig. 5** Biomass production at the end of the experiment (mean value and standard error).
755 Different letter indicate differences according to Tukey´s HSD test at a probability level

of 0.05. 5C: unflooded mesocosms at 5 °C; 15C: unflooded mesocosms at 15 °C; 25C: unflooded mesocosms at 25 °C; 5F: flooded mesocosms at 5 °C; 15F: flooded mesocosms at 15 °C; 25F: flooded mesocosms at 25 °C. Four replicates per treatment.

Highlights

- Flooding induced a rapid release of nutrients, especially at higher temperatures.
- 700 kg CH_4-C ha^{-1} and 5 kg NH_3-N ha^{-1} were released in the flood phase at 25 °C.
- During soil recovery, nitrification led to 1.0-14.2 kg N_2O-N ha^{-1} losses at 5-25 °C.
- Flooding reduced soil microbial biomass, actinomycetes and arbuscular mycorrhiza.
- Flooding reduced biomass production by 18% at 5 °C, 50% at 15 °C and 95% at 25 °C.

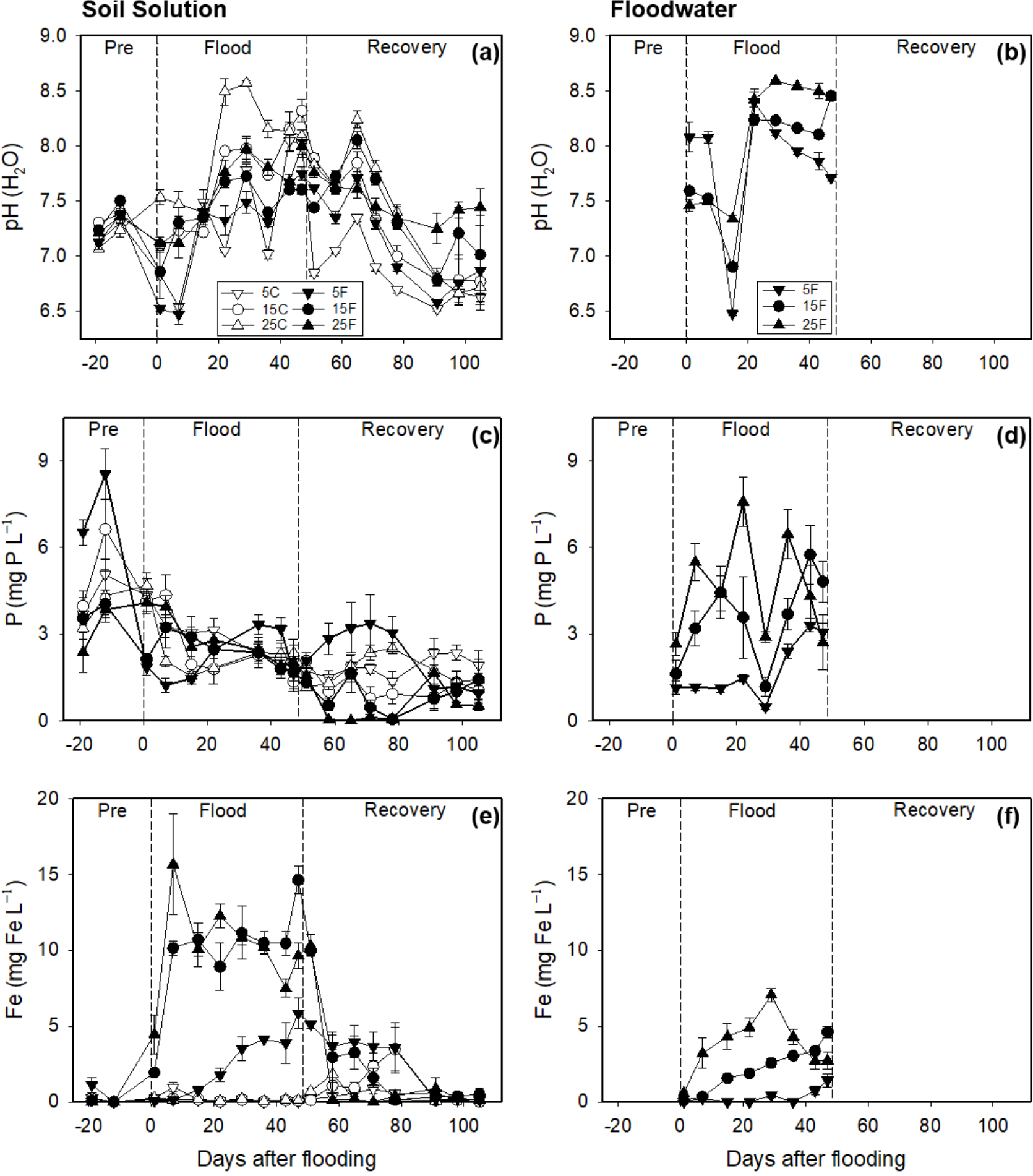
Soil Solution
Floodwater
Pre
Flood
Recovery
(a)
(b)
(c)
(d)
(e)
(f)
pH (H2O)
P (mg P L-1)
Fe (mg Fe L-1)
5C
15C
25C
5F
15F
25F
Days after flooding

Fig. 1

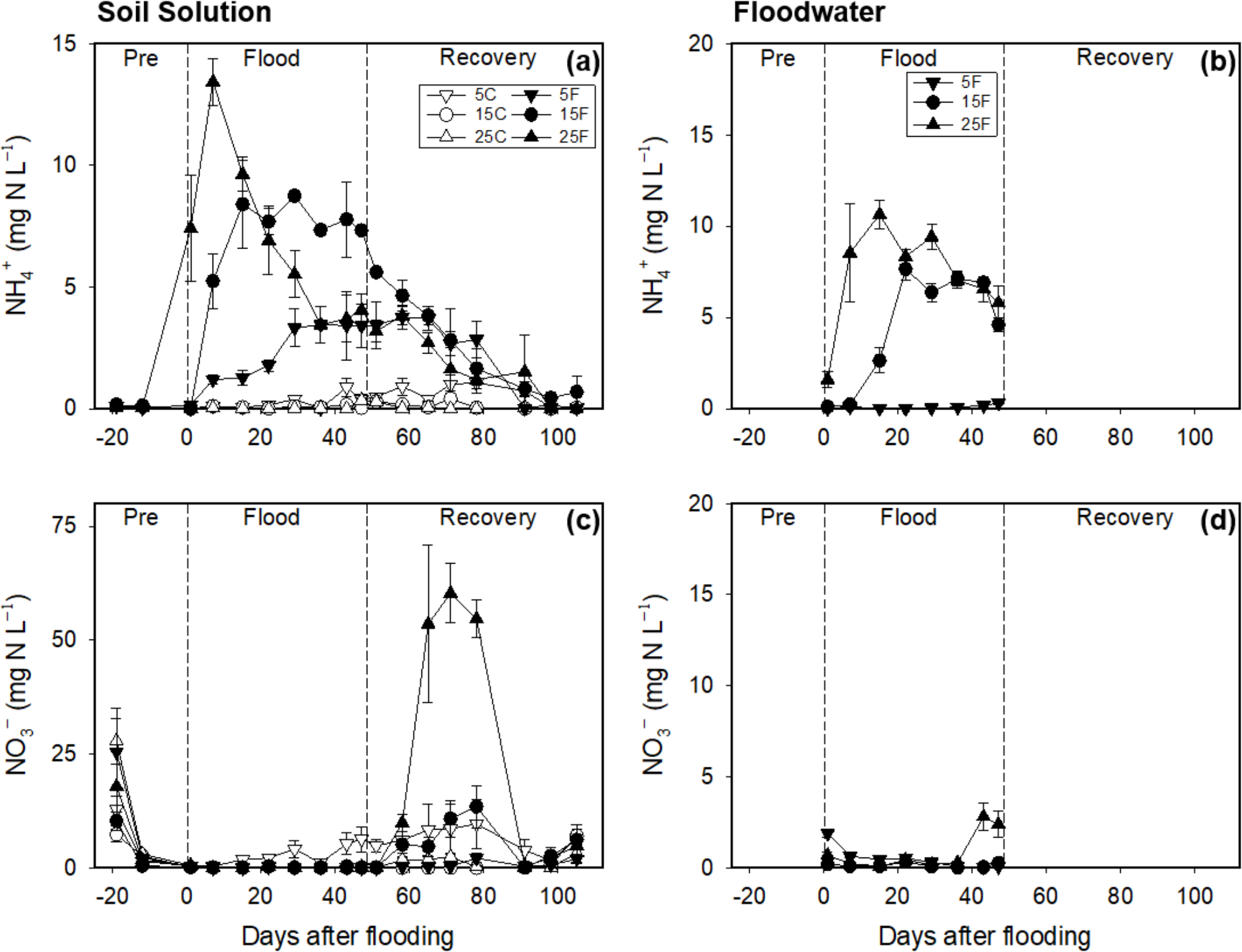
Soil Solution
Floodwater
Pre
Flood
Recovery
(a)
(b)
(c)
(d)
5C
15C
25C
5F
15F
25F
NH_4^+ (mg N L^{-1})
NO_3^- (mg N L^{-1})
Days after flooding

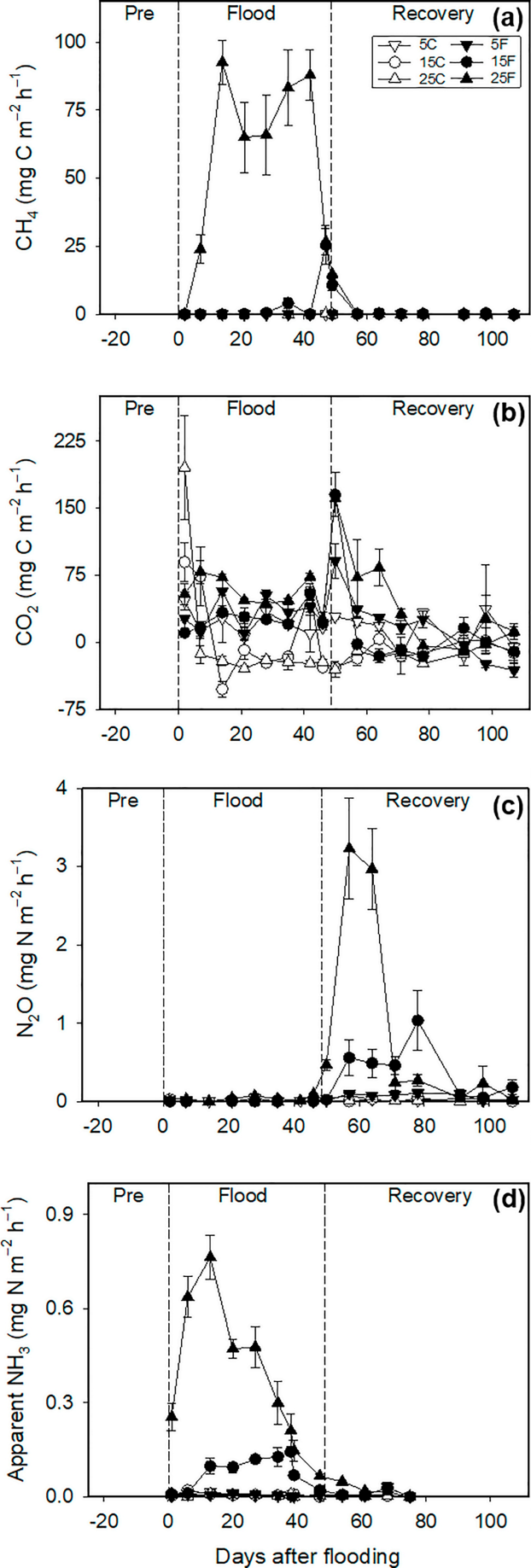
Pre
Flood
Recovery
(a)
5C
15C
25C
5F
15F
25F
CH4 (mg C m-2 h-1)
100
75
50
25
0
-20
0
20
40
60
80
100
(b)
CO2 (mg C m-2 h-1)
225
150
75
0
-75
(c)
N2O (mg N m-2 h-1)
4
3
2
1
0
(d)
Apparent NH3 (mg N m-2 h-1)
0.9
0.6
0.3
0.0
Days after flooding

Taxonomic groups and environmental variables

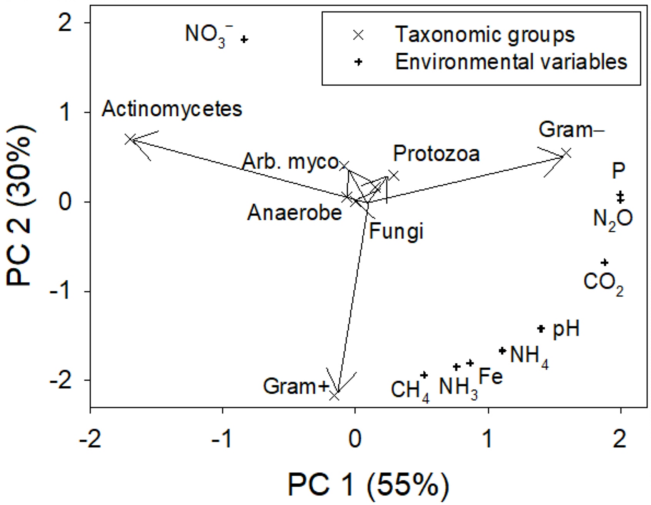

After the flood phase

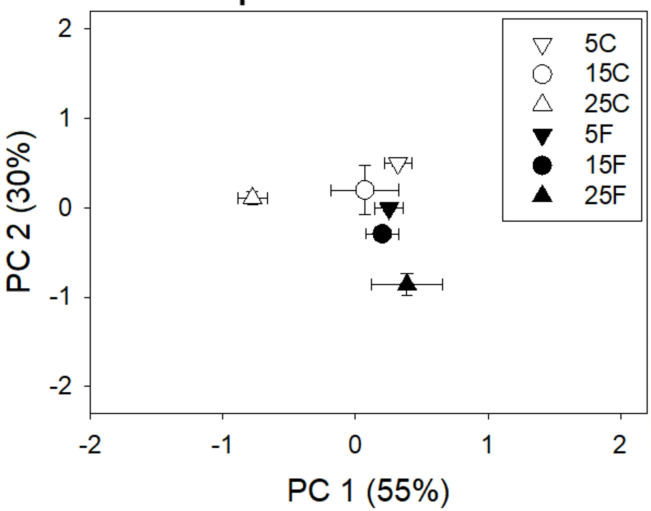

After the soil recovery

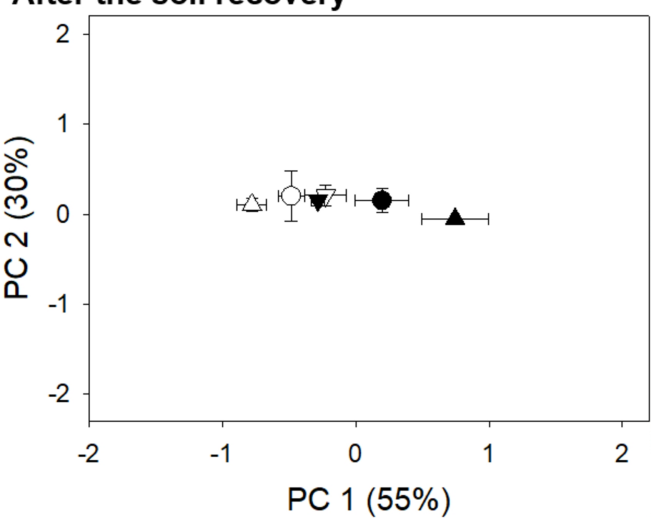

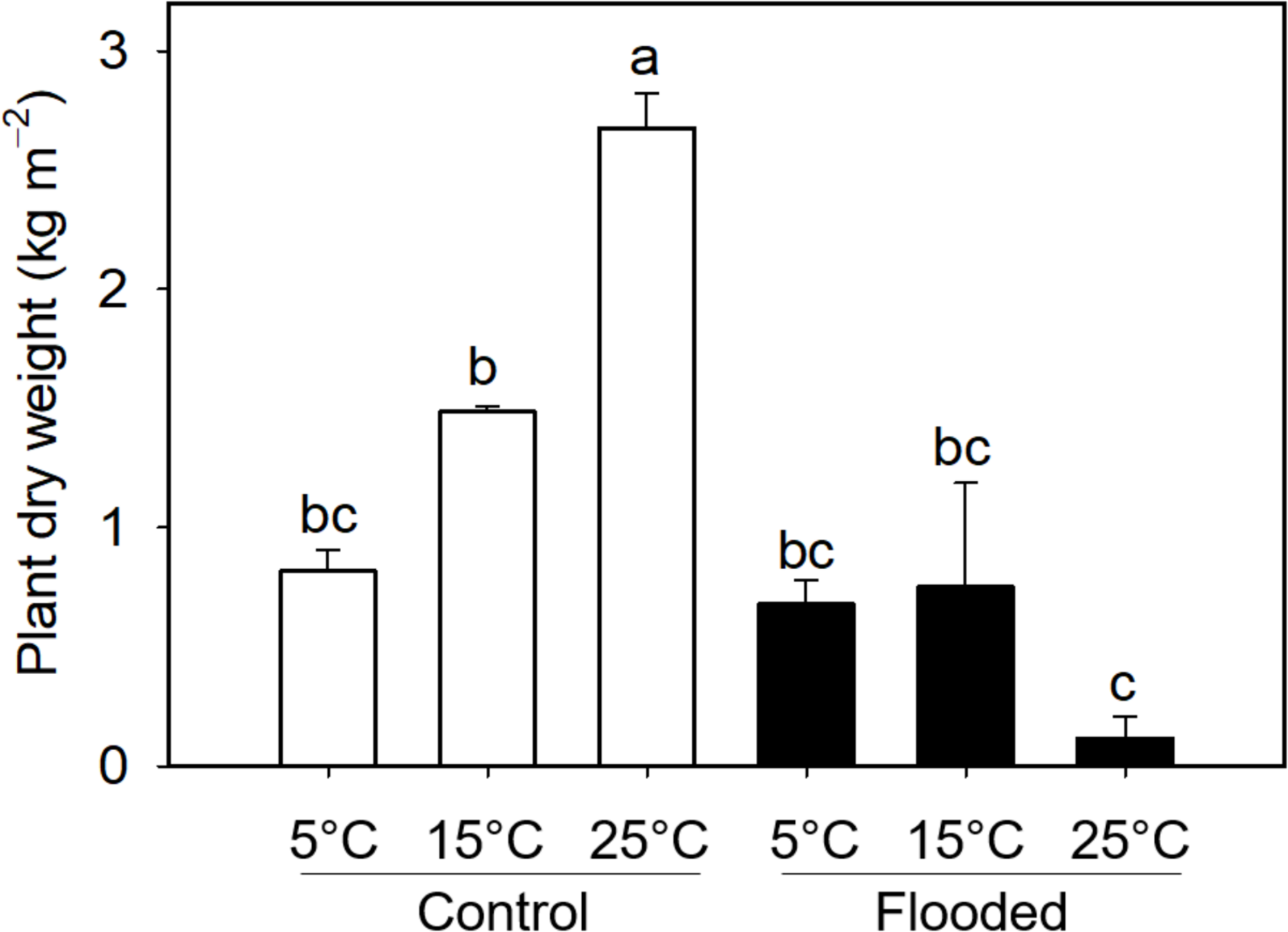
Plant dry weight (kg m^{-2})
3
2
1
0
a
b
bc
bc
bc
c
5°C
15°C
25°C
5°C
15°C
25°C
Control
Flooded

Table 1 Potential losses of nutrients (mean ± standard error, $n = 4$) as a function of temperature and flooding. Different letters indicate differences according to Tukey's HSD test at a probability level of 0.05.

Treatment	P (kg P ha^{-1})	Fe (kg Fe ha^{-1})	NH_4^+ (kg N ha^{-1})	NO_3^- (kg N ha^{-1})
Control 5°C	1.9 ± 0.1 c	0.4 ± 0.1 d	0.4 ± 0.1 d	3.6 ± 1.0 a
Control 15°C	1.9 ± 0.1 c	0.0 ± 0.0 d	0.1 ± 0.0 d	0.2 ± 0.0 b
Control 25°C	1.9 ± 0.2 c	0.1 ± 0.0 d	0.1 ± 0.0 d	0.2 ± 0.1 b
Flood 5°C	5.0 ± 0.2 b	3.9 ± 0.6 c	2.4 ± 0.4 c	2.0 ± 0.2 ab
Flood 15°C	8.5 ± 0.4 a	10.6 ± 0.4 b	12.5 ± 0.2 b	0.5 ± 0.1 b
Flood 25°C	9.6 ± 0.7 a	13.7 ± 1.3 a	17.3 ± 1.0 a	3.6 ± 0.7 a
P value	**<0.001**	**<0.001**	**<0.001**	**<0.001**

Table 2 Cumulative GHG fluxes, global warming potential (GWP in equivalent kg of CO_2) and apparent NH_3 volatilization (mean ± standard error, $n = 4$) as a function of temperature and flooding. Different letters indicate differences according to Tukey's HSD test at a probability level of 0.05.

Treatment	CH_4 (kg C ha^{-1})	CO_2 (kg C ha^{-1})	N_2O (kg N ha^{-1})	GWP (kg C ha^{-1})	GWP* (kg C ha^{-1})	Apparent NH_3 (kg N ha^{-1})
Control 5°C	0.5 ± 0.6 c	421 ± 79 b	0.6 ± 0.2 cd	614 ± 51 b	192 ± 66 b	0.1 ± 0.0 c
Control 15°C	0.8 ± 0.8 c	−73 ± 65 c	0.0 ± 0.2 d	−33 ± 83 b	41 ± 43 b	0.1 ± 0.0 c
Control 25°C	−0.2 ± 0.5 c	−289 ± 60 c	−0.1 ± 0.1 d	−311 ± 94 b	−22 ± 45 b	0.1 ± 0.0 c
Flood 5°C	0.3 ± 0.2 c	595 ± 74 b	1.0 ± 0.1 c	896 ± 116 b	301 ± 49 b	0.1 ± 0.0 c
Flood 15°C	45.7 ± 5.2 b	453 ± 88 b	5.7 ± 1.4 b	3713 ± 519 b	3261 ± 435 b	1.0 ± 0.9 b
Flood 25°C	717.7 ± 75.5 a	1196 ± 102 a	14.2 ± 1.9 a	29817 ± 2162 a	28621 ± 2267 a	5.0 ± 0.2 a
P value	**<0.001**	**<0.001**	**<0.001**	**<0.001**	**<0.001**	**<0.001**

GWP*: global warming potential excluding CO_2 emissions.

Table 3 ANOVA of soil microbial biomass (total amount of PLFAs, nmol g^{-1}) and taxonomic groups (%) at the end of the flood phase and after floodwater removal and soil recovery (mean ± standard error, $n = 4$). Different letters indicate differences according to Tukey's HSD test at a probability level of 0.05.

Treatment	Microbial biomass (nmol g^{-1})	Gram+ bacteria (%)	Gram− bacteria (%)	Actinomycetes (%)	Anaerobes (%)	Protozoa (%)	Arb. myco. (%)	Fungi (%)
At the end of flooding								
Control 5°C	379.5 ± 32.9 a	24.3 ± 0.2 c	49.6 ± 0.2	14.2 ± 0.4 ab	1.61 ± 0.09	2.17 ± 0.12	6.36 ± 0.13 a	1.85 ± 0.39 ab
Control 15°C	339.1 ± 17.5 a	25.6 ± 1.3 bc	48.3 ± 1.1	14.6 ± 0.5 ab	1.64 ± 0.15	2.18 ± 0.34	5.70 ± 0.23 ab	2.00 ± 0.16 a
Control 25°C	311.9 ± 8.2 a	27.1 ± 0.2 b	47.0 ± 0.5	16.3 ± 0.4 a	1.55 ± 0.16	2.00 ± 0.08	4.95 ± 0.14 bc	1.15 ± 0.23 abc
Flood 5°C	378.9 ± 23.3 a	26.5 ± 0.2 bc	48.9 ± 0.4	13.7 ± 0.4 b	1.31 ± 0.09	1.96 ± 0.04	6.34 ± 0.21 a	1.19 ± 0.10 abc
Flood 15°C	342.2 ± 21.4 a	27.7 ± 0.3 ab	48.8 ± 0.5	13.8 ± 0.3 b	1.78 ± 0.09	1.86 ± 0.07	5.28 ± 0.15 b	0.83 ± 0.13 c
Flood 25°C	183.4 ± 18.8 b	30.2 ± 0.6 a	48.8 ± 1.1	12.5 ± 0.8 b	1.34 ± 0.07	1.87 ± 0.12	4.34 ± 0.29 c	0.93 ± 0.13 bc
P value	**<0.001**	**<0.001**	0.242	**0.002**	0.063	0.598	**<0.001**	**0.004**
After soil recovery								
Control 5°C	306.0 ± 27.6 a	25.7 ± 0.5 a	47.8 ± 0.6 bc	16.0 ± 0.5 ab	1.41 ± 0.07 b	2.20 ± 0.11 ab	5.25 ± 0.13 a	1.60 ± 0.40 ab
Control 15°C	242.0 ± 5.4 ab	26.0 ± 0.1 a	47.5 ± 0.3 bc	17.3 ± 0.5 ab	1.48 ± 0.09 ab	1.99 ± 0.14 ab	4.94 ± 0.24 a	0.85 ± 0.21 ab
Control 25°C	269.0 ± 12.4 a	27.3 ± 0.3 ab	46.0 ± 0.6 c	17.7 ± 0.2 a	1.93 ± 0.10 a	2.01 ± 0.11 ab	4.43 ± 0.16 ab	0.64 ± 0.08 b
Flood 5°C	271.3 ± 4.3 a	26.1 ± 0.2 a	48.0 ± 0.3 bc	16.4 ± 0.1 ab	1.50 ± 0.16 ab	1.75 ± 0.05 b	5.23 ± 0.07 a	1.05 ± 0.19 ab
Flood 15°C	269.4 ± 16.7 a	26.0 ± 0.5 ab	49.8 ± 0.7 ab	15.0 ± 0.9 bc	1.46 ± 0.06 b	2.01 ± 0.18 ab	4.62 ± 0.18 ab	1.12 ± 0.27 ab
Flood 25°C	179.3 ± 6.7 b	26.6 ± 0.1 b	51.1 ± 0.9 a	12.9 ± 0.8 c	1.29 ± 0.09 b	2.57 ± 0.26 a	3.50 ± 0.45 b	2.03 ± 0.39 a
P value	**<0.001**	0.052	**<0.001**	**<0.001**	**0.006**	**0.032**	**0.003**	**0.025**

Control: mesocosms without flooding; Flood: mesocosms which were flooded.
Anaerobes anaerobic bacteria, *Arb. Myco. putative* arbuscular mycorrhizal fungi.